

Estimation of magnetic field mapping accuracy using the pulsating aurora-chorus connection

Y. Nishimura,^{1,2} J. Bortnik,¹ W. Li,¹ R. M. Thorne,¹ L. R. Lyons,¹ V. Angelopoulos,³ S. B. Mende,⁴ J. Bonnell,⁴ O. Le Contel,⁵ C. Cully,⁶ R. Ergun,⁷ and U. Auster⁸

Received 26 May 2011; revised 9 June 2011; accepted 10 June 2011; published 27 July 2011.

[1] Although magnetic field models are widely used in magnetosphere-ionosphere coupling studies to perform field-line mapping, their accuracy has been difficult to estimate experimentally. Taking advantage of the high correlation between lower-band chorus and pulsating aurora, we located the THEMIS spacecraft footprint within \sim km accuracy and calculated the differences from mappings given in widely-used Tsyganenko models. Using 13 conjunctions of the THEMIS spacecraft and ground-based imagers, we found that the Tsyganenko model footprints were located within 1° – 2° magnetic latitude and 0.1–0.2 h magnetic local time of our derived footprint. The deviation between the footprints has a consistent dependence on geomagnetic activity. Our results showed that the real magnetic field tends to be less stretched than that in the Tsyganenko models during quiet times and comparable to or more stretched during disturbed times. This approach can be used to advance modeling of field lines that connect to the near-Earth plasma sheet. **Citation:** Nishimura, Y., et al. (2011), Estimation of magnetic field mapping accuracy using the pulsating aurora-chorus connection, *Geophys. Res. Lett.*, 38, L14110, doi:10.1029/2011GL048281.

1. Introduction

[2] Magnetic field mapping is a crucial part of magnetospheric and ionospheric studies. A series of practical, empirical models [Tsyganenko, 2010, and references therein] that include effects of magnetospheric currents and give associated field line stretching have been widely used to successfully connect large- and meso-scale (several hundred kilometers in the ionosphere) structures of particles, aurora, and plasma flows at two different altitudes at magnetically connected locations [e.g., Wygant et al., 2000; Marchaudon

et al., 2004; Dombek et al., 2005]. Such magnetic field maps have been validated based on striking similarities in flow pattern or particle distribution along magnetic field lines [Weiss et al., 1997; Puhl-Quinn et al., 2007]. Conjugate auroral measurements are also useful for highlighting magnetic conjugate locations in each hemisphere [Sato et al., 2005; Motoba et al., 2010]. Also useful are event-oriented magnetic field reconstructions [e.g., Pulkkinen, 1991; Kubyshkina et al., 2011], which can reproduce measured in-situ magnetic fields but are limited by spacecraft coverage.

[3] Higher accuracy is required for mapping of smaller-scale (\sim 100 or fewer kilometers in the ionosphere) phenomena, which are of particular importance for connecting the auroral ionosphere and the magnetotail. Such accuracy is extremely difficult to achieve, however, due to highly variable external currents and the dynamic nature of auroral forms. Thus, experimental validation of the magnetic field configuration is needed for reliable mapping.

[4] Nishimura et al. [2010] proposed a method to determine the precise magnetic footprint of a magnetic field line threading a spacecraft in the plasma sheet with an accuracy of \sim a few kilometers in the ionosphere. Using conjugate measurements by the THEMIS spacecraft and all-sky imager (ASI), they showed a high correlation between the intensity modulation of lower-band chorus waves measured in space and the pulsating aurora (PA) observed by an ASI on the ground. This correlation, which has been observed consistently during spacecraft-imager conjunctions in multiple events (Y. Nishimura et al., Multi-event study of pulsating aurora-chorus correlation, submitted to *Journal of Geophysical Research*, 2011), shows that PA results from electron scattering by the observed chorus. Taking advantage of the spatial scale of the PA patches and the fact that adjacent patches pulsate incoherently with one another, the small area of the sky that correlates with the chorus wave locates the real magnetic footprint of the spacecraft independent of any magnetic field model. The accuracy of various magnetic field models can thus be estimated by comparing their predicted footprints against our observed footprint location.

[5] In the present study, we used 13 conjunctions (Nishimura et al., submitted manuscript, 2011) between the THEMIS spacecraft and ASIs [Angelopoulos, 2008; Mende et al., 2008] from 2007 to 2010 to determine typical differences between the highest-correlation area and model footprints. We only chose cases in which the spacecraft detected intense (>10 pT) lower-band chorus in the particle burst mode and conjugate auroral observations were available near a model magnetic footprint. The imager data were mapped onto a 110 km altitude plane. This approach is valid over a wide elevation angle range without much distortions because the pulsating aurora occurs in a narrow altitude range, with

¹Department of Atmospheric and Oceanic Sciences, University of California, Los Angeles, California, USA.

²Solar-Terrestrial Environment Laboratory, Nagoya University, Nagoya, Japan.

³Institute of Geophysics and Planetary Physics, University of California, Los Angeles, California, USA.

⁴Space Sciences Laboratory, University of California, Berkeley, California, USA.

⁵Laboratoire de Physique des Plasmas, CNRS/Ecole Polytechnique/UPMC/Paris-Sud 11, Saint-Maur-des-Fossés, France.

⁶Swedish Institute of Space Physics, Uppsala, Sweden.

⁷Laboratory for Atmospheric and Space Physics, University of Colorado at Boulder, Boulder, Colorado, USA.

⁸Institut für Geophysik und Extraterrestrische Physik, Technischen Universität Braunschweig, Braunschweig, Germany.

Table 1. Deviations of the Model Footprints Relative to the Highest Correlation Location^a

Event	Date	S/C Time Name	R, MLT, MLAT		MLAT (deg)				MLT (h)				Magnetic Condition		
			R	MLT	T89	T96	T02	T05s	IGRF	T89	T96	T02		T05s	
a	20081109	0627	e	5.3, 4.6, 5.8	1.38	0.80	1.34	1.62	-0.05	-0.06	-0.01	-0.07	recovery	-65, -10	
b	20081207	0556	e	7.0, 3.7, 5.0	-1.40	-1.80	-1.23	-0.99	-0.16	-0.19	-0.13	-0.32	expansion	-47, -51	
c	20090215	0111	a	6.9, 22.8, -0.3	0.55	-0.55	0.01	0.67	0.10	0.09	0.10	0.16	expansion	3, 84	
d	20090215	0138	e	7.0, 22.8, 4.2	3.16	0.83	0.26	0.93	0.07	0.06	0.04	0.13	recovery	-3, 80	
e	20090215	0144	a	7.5, 23.1, -0.3	0.00	-1.22	-0.64	0.11	0.14	0.13	0.11	0.19	recovery	-95, -113	
f	20100106	0531	d	8.5, 4.1, 3.1	-1.47	-1.54	-1.17	-0.87	-0.12	-0.19	-0.04	-0.38	quiet	4, -2	
g	20100106	0617	e	9.2, 4.5, 4.1	-2.21	-1.52	-1.47	-1.27	-0.24	-0.28	-0.12	-0.32	quiet	12, 22	
h	20100106	0637	d	8.6, 4.2, 4.5	-2.09	-1.17	-1.18	-1.11	-0.11	-0.14	-0.07	-0.19	quiet	5, 14	
i	20100114	0508	d	8.5, 3.5, 3.4	-2.65	-2.54	-2.20	-1.75	-0.34	-0.41	-0.21	-0.48	quiet	-16, -17	
j	20100204	0349	e	8.2, 1.9, 3.3	2.83	0.32	0.41	0.97	-0.44	-0.49	-0.38	-0.55	quiet	21, 20	
k	20100306	0154	d	8.2, 0.2, 3.3	3.52	0.83	1.02	1.30	0.03	-0.01	0.09	0.02	recovery	21, 40	
l	20100306	0154	e	8.0, 0.1, 3.3	3.39	0.74	0.92	1.18	-0.12	-0.15	-0.06	-0.13	recovery	21, 40	
m	20100306	0213	d	8.5, 0.3, 3.8	1.63	-1.13	-0.95	-0.53	-0.24	-0.27	-0.17	-0.23	quiet	31, 60	
quiet	-	-	-	-	0.58 ± 1.12	-1.79 ± 0.94	-1.34 ± 0.93	-1.17 ± 0.85	-0.99 ± 0.94	-0.24 ± 0.13	-0.27 ± 0.13	-0.31 ± 0.13	-0.14 ± 0.12	-0.35 ± 0.14	-
median	-	-	-	-	2.71 ± 1.01	0.54 ± 0.87	-0.24 ± 1.05	0.26 ± 0.94	0.93 ± 0.88	0.03 ± 0.11	-0.01 ± 0.12	0.05 ± 0.16	0.04 ± 0.09	0.02 ± 0.18	-
disturbed	-	-	-	-	-	-	-	-	-	-	-	-	-	-	-
median	-	-	-	-	-	-	-	-	-	-	-	-	-	-	-

^aThe spacecraft locations in the 3rd column are given for R [R_E], MLT [h] and MLAT [deg]. The magnetic condition is based on the magnetic field measured on the Greenland sector (expansion: increasing or steady magnetic disturbance, recovery: decreasing magnetic disturbance, quiet: small deviation from daily mean). H and Z component at Narsarsuaq are also shown in nT.

a vertical extent of less than 2 km [Stenbaek-Nielsen and Hallinan, 1979]. The location with the highest cross-correlation between auroral emissions and intensity modulation of lower-band chorus was determined for each event by calculating two-dimensional cross correlation coefficients. The high correlation region is confined to a patch area (~a few kilometers) because a patch changes its shape in time and surrounding patches have different phases and periods of pulsation [Nishimura et al., 2010]. The highest correlation location was compared to model footprints estimated by the T89 [Tsyganenko, 1989], T96 [Tsyganenko, 1995, 1996], T02 [Tsyganenko, 2002], and TS05s [Tsyganenko and Sitnov, 2005] models, and for reference, to the International Geomagnetic Reference Field 11th (IGRF-11) [Finlay et al., 2010] model, which does not include external current effects. The spacecraft distributed at 5.3–9.2 R_E, 22.8–4.6 h MLT and -0.3°–5.8° MLAT.

2. Results

[6] A typical conjunction event (event h in Table 1) is shown in Figure 1. The intensity of lower-band chorus is modulated quasi-periodically with a recurrence period of ~10–20 s (Figures 1a and 1b); the upper-band chorus and electron cyclotron harmonic (ECH) waves are much weaker or negligible. The ASI keogram at Narsarsuaq (Figure 1c,

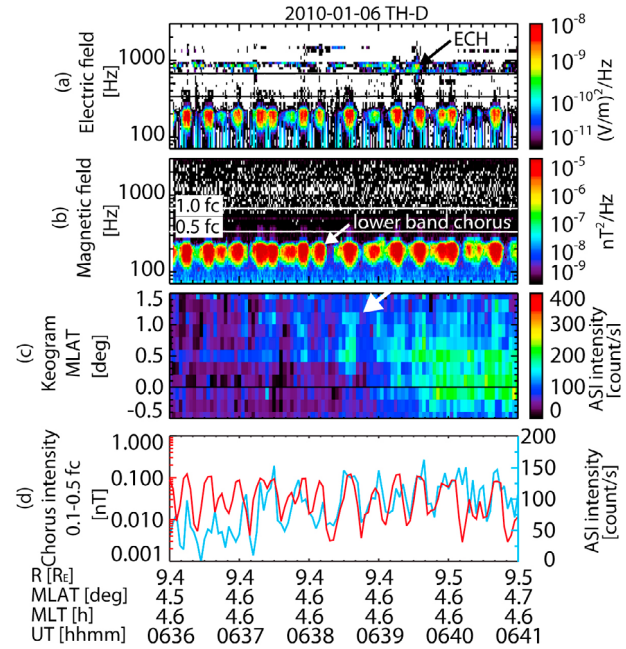


Figure 1. THEMIS-D (TH-D) spacecraft and imager conjunction event on 6 January 2010. Time series of electromagnetic field wave intensity, ASI keogram at longitudes including a highest correlation PA patch, a comparison between the frequency-integrated wave magnetic field intensity from 0.1 to 0.5 electron cyclotron frequencies (f_c) down-sampled to the 3-sec ASI resolution, and ASI intensity at the highest-correlating latitude indicated by the white arrow in the keogram. The black and white lines in the top two panels show 1.0 and 0.5 f_c . The vertical axis of the keograms is given by the latitude relative to the T02 footprint.

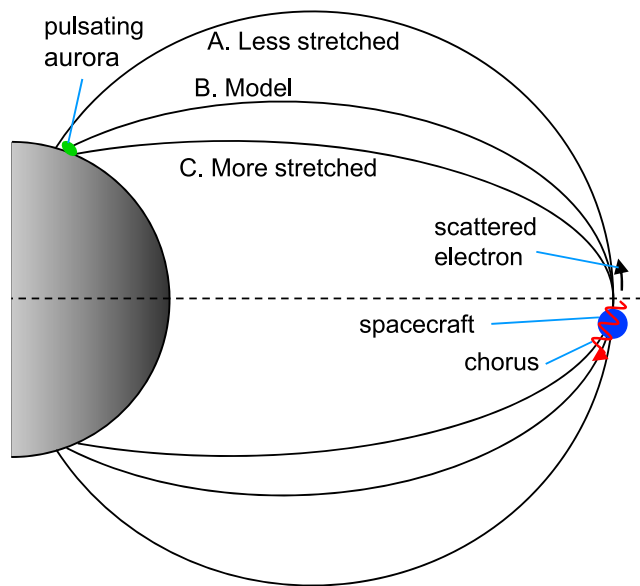


Figure 2. Schematic illustration of the magnetic field configuration, which can be estimated by the chorus-PA correlation. The chorus-PA correlation highlights the footprint of the field line threading the spacecraft. Deviation of the footprint from a model footprint location indicates a degree of stretching relative to the model field line.

61.16° and 314.56° in geographic latitude and longitude) shows that the PA was located poleward of the T02 model footprint latitude. The chorus intensity is highly correlated with the PA, as shown in Figure 1d, and the actual magnetic footprint of the spacecraft is thus located slightly poleward of the T02 footprint. When the PA patch size is ~100 km, the footprint location can be determined with a much higher accuracy, because the patch changes its location and shape with time. This property allows us to determine the highest correlation location, which is much smaller (a few km) than the patch size and lies 1.2° above the T02 footprint latitude for this event. As shown schematically in Figure 2, the more poleward footprint indicates a magnetic field configuration that is less stretched than the model field line.

[7] The same analysis was performed for the other events (7 of which have been presented by *Nishimura et al.* [2010, submitted manuscript, 2011]). Deviations from the magnetic field models are listed in Table 1 and shown in Figure 3. On average, the newer Tsyganenko models (T96, T02 and T05s) give footprint locations within ~1° in magnetic latitude (MLAT) and 0.1–0.2 h in magnetic local time (MLT) (events a, c, d, e and k–m). The deviation in the 2-d plane of the ionosphere is the smallest for the T02 model (1.02° in MLAT and 0.09 h in MLT). In a statistical sense, T02 thus gives the best estimate of the magnetic footprint of the spacecraft in the PA regions. This result would be because T02 contains more realistic current distributions than T89 and T96. T02 is also a function of preceding solar wind parameters. T05s is tuned for storm-time magnetic field

modeling and may not accurately reproduce the magnetic field during the non-storm times.

[8] By categorizing our event list according to magnetic activity level, a more consistent bias tends to emerge in the magnetic field models. During magnetically quiet times (Figure 3a), the “real” footprint (derived from the chorus-ASI highest correlation pixel) tends to be located between the Tsyganenko and IGRF model footprints in latitude, indicating that the model fields are too stretched (see field lines A and B in Figure 2). The real footprints are located ~1° MLAT poleward of the Tsyganenko model latitudes. Here quiet time means a time period with a small deviation of the ground magnetic field from the daily mean at the ASI location. The substorm growth phase is not included in our conjunction events, perhaps because PA occurs preferentially after substorm onset.

[9] During disturbed conditions (substorm expansion and recovery phases, Figure 3b), on the other hand, the model footprints tend to cluster close to or slightly higher in latitude than the real footprint, indicating that model field stretching tends to be approximately correct or possibly slightly insufficient (field lines B and C in Figure 2). The real footprints are located on average ~0.5° MLAT equatorward of the Tsyganenko model latitudes. This tendency is similar to the finding from an event-oriented model [*Kubyshkina et al.*, 2011], and indicates that the real magnetic field tends to be less stretched than in the Tsyganenko models during quiet times and comparable to or more stretched during disturbed times. The MLT difference is less than ~0.05 h, and thus well reproduced in the model fields.

[10] The latitudinal locations of the real footprint relative to the model footprints are roughly consistent with the in-situ magnetic field compared to the model fields (not shown). The quiet-time magnetic field inclination is closer to that of IGRF, while the inclination during the disturbed times tends to be close to that of T02. This tendency gives a support for our study that the PA mapping reflects the actual magnetic field geometry.

3. Summary

[11] The high correlation between lower-band chorus and PA was utilized to estimate the accuracy of several widely-used magnetic field models. Using 13 events of conjugate THEMIS spacecraft and ground-based imager measurements during periods of intense lower-band chorus waves, we found that the Tsyganenko magnetic field models give reasonable estimates of the spacecraft footprint within 1–2° MLAT and 0.1–0.2 h MLT. The deviation between the highest-correlation pixel and model footprints shows dependence on geomagnetic activity; the Tsyganenko models tend to overestimate field-line stretching during quiet times, and to be approximately correct or understretched during active times. The MLT is generally well explained by the models. Note, however, that our analysis is limited to the PA occurrence region, near the equatorward boundary of the auroral oval mainly at postmidnight after substorm onset. Model accuracy is likely to change in different regions and for different magnetic conditions. Nevertheless, our results will be useful for magnetosphere-ionosphere coupling studies and will provide future opportunities to advance magnetic field modeling.

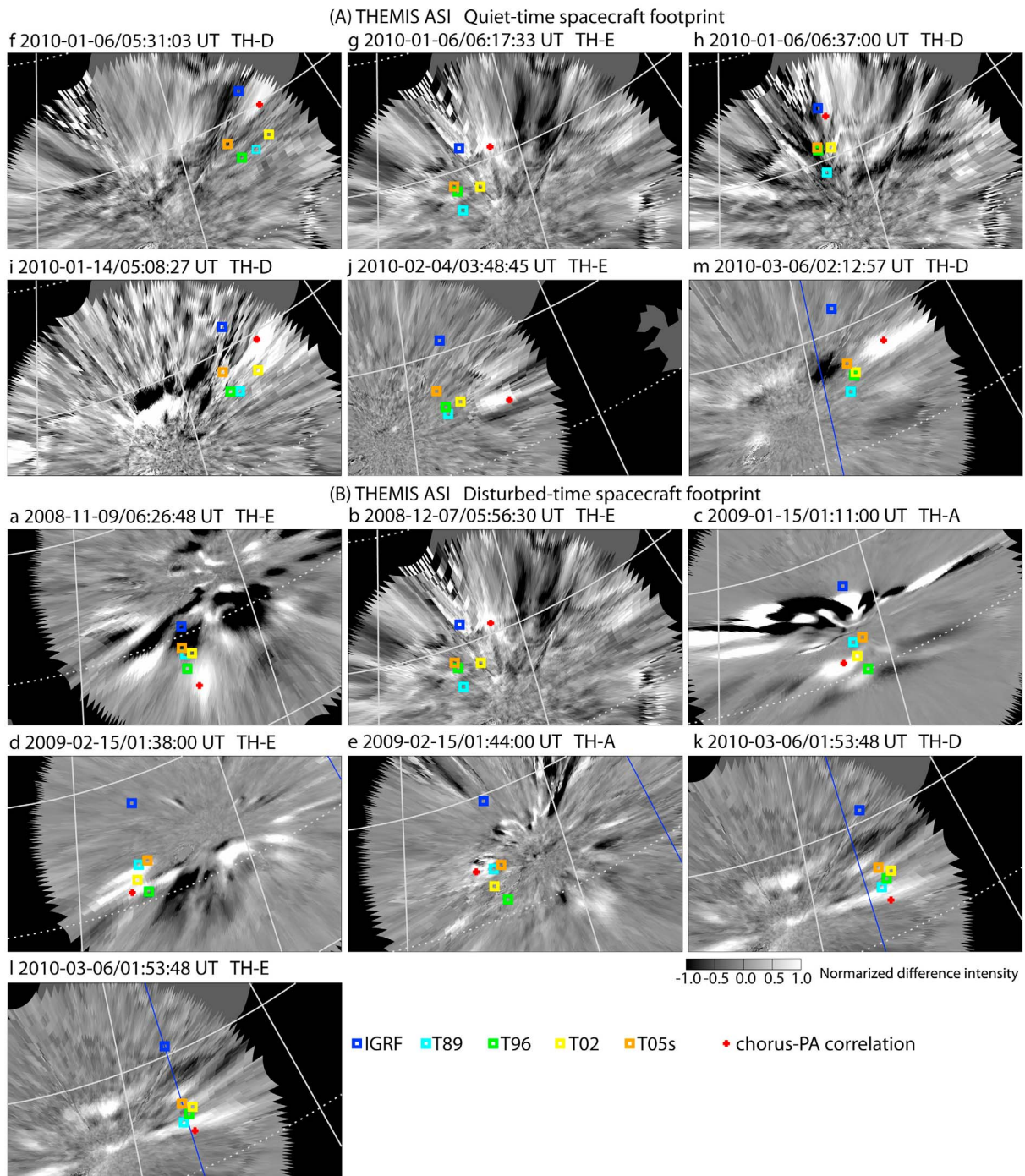


Figure 3. Comparison between location of highest-correlation pixels of the ASI with chorus intensity (red) and spacecraft magnetic footprints of the spacecraft (TH-A, D or E) using IGRF, T89, T96, T02 and T05s overlain on difference auroral images (difference between the current and previous frame). White lines are isocontours of magnetic latitude (every 10° in solid lines) and longitude (every 15°). The blue line shows the magnetic midnight meridian. (a) For quiet time and (b) disturbed time events.

[12] **Acknowledgments.** This work was supported by NASA contract NAS5-02099, 9F007-046101, NSF grants ATM-0802843 and AGS-0840178, and JSPS Research Fellowship.

[13] The Editor thanks Tetsuo Motoba and an anonymous reviewer for their assistance in evaluating this paper.

References

- Angelopoulos, V. (2008), The THEMIS mission, *Space Sci. Rev.*, *141*, 5–34, doi:10.1007/s11214-008-9336-1.
- Dombeck, J., C. Cattell, J. R. Wygant, A. Keiling, and J. Scudder (2005), Alfvén waves and Poynting flux observed simultaneously by Polar and FAST in the plasma sheet boundary layer, *J. Geophys. Res.*, *110*, A12S90, doi:10.1029/2005JA011269.
- Finlay, C., et al. (2010), International Geomagnetic Reference Field: The eleventh generation, *Geophys. J. Int.*, *183*(3), 1216–1230, doi:10.1111/j.1365-246X.2010.04804.x.
- Kubyskhina, M., V. Sergeev, N. Tsyganenko, V. Angelopoulos, A. Runov, E. Donovan, H. Singer, U. Auster, and W. Baumjohann (2011), Time-dependent magnetospheric configuration and breakup mapping during a substorm, *J. Geophys. Res.*, *116*, A00I27, doi:10.1029/2010JA015882.
- Marchaudon, A., et al. (2004), Transient plasma injections in the dayside magnetosphere: One-to-one correlated observations by Cluster and SuperDARN, *Ann. Geophys.*, *22*, 141–158, doi:10.5194/angeo-22-141-2004.
- Mende, S. B., et al. (2008), The THEMIS array of ground-based observatories for the study of auroral substorms, *Space Sci. Rev.*, *141*, 357–387, doi:10.1007/s11214-008-9380-x.
- Motoba, T., K. Hosokawa, N. Sato, A. Kadokura, and G. Björnsson (2010), Varying interplanetary magnetic field By effects on interhemispheric conjugate auroral features during a weak substorm, *J. Geophys. Res.*, *115*, A09210, doi:10.1029/2010JA015369.
- Nishimura, Y., et al. (2010), Identifying the driver of pulsating aurora, *Science*, *330*(6000), 81–84, doi:10.1126/science.1193186.
- Puhl-Quinn, P. A., H. Matsui, E. Mishin, C. Moukikis, L. Kistler, Y. Khotyaintsev, P. M. E. Décréau, and E. Lucek (2007), Cluster and DMSP observations of SAID electric fields, *J. Geophys. Res.*, *112*, A05219, doi:10.1029/2006JA012065.
- Pulkkinen, T. I. (1991), A study of magnetic field and current configurations in the magnetotail at time of a substorm onset, *Planet. Space Sci.*, *39*, 833–845, doi:10.1016/0032-0633(91)90088-R.
- Sato, N., A. Kadokura, Y. Ebihara, H. Deguchi, and T. Saemundsson (2005), Tracing geomagnetic conjugate points using exceptionally similar synchronous auroras, *Geophys. Res. Lett.*, *32*, L17109, doi:10.1029/2005GL023710.
- Stenback-Nielsen, H., and T. Hallinan (1979), Pulsating auroras: Evidence for noncollisional thermalization of precipitating electrons, *J. Geophys. Res.*, *84*, 3257–3271, doi:10.1029/JA084iA07p03257.
- Tsyganenko, N. A. (1989), A magnetospheric magnetic field model with a warped tail current sheet, *Planet. Space Sci.*, *37*, 5–20, doi:10.1016/0032-0633(89)90066-4.
- Tsyganenko, N. A. (1995), Modeling the Earth’s magnetospheric magnetic field confined within a realistic magnetopause, *J. Geophys. Res.*, *100*, 5599–5612, doi:10.1029/94JA03193.
- Tsyganenko, N. A. (1996), Effects of the solar wind conditions on the global magnetospheric configuration as deduced from data-based field models, in *Third International Conference on Substorms, Versailles, France, 12–17 May 1996*, edited by E. J. Rolfe and B. Kaldeich, *Eur. Space Agency Spec. Publ., ESA SP-389*, 181–185.
- Tsyganenko, N. A. (2002), A model of the near magnetosphere with a dawn-dusk asymmetry: 1. Mathematical structure, *J. Geophys. Res.*, *107*(A8), 1179, doi:10.1029/2001JA000219.
- Tsyganenko, N. A. (2010), On the reconstruction of magnetospheric plasma pressure distributions from empirical geomagnetic field models, *J. Geophys. Res.*, *115*, A07211, doi:10.1029/2009JA015012.
- Tsyganenko, N. A., and M. I. Sitnov (2005), Modeling the dynamics of the inner magnetosphere during strong geomagnetic storms, *J. Geophys. Res.*, *110*, A03208, doi:10.1029/2004JA010798.
- Weiss, L. A., R. Lambour, R. Elphic, and M. Thomsen (1997), Study of plasmaspheric evolution using geosynchronous observations and global modeling, *Geophys. Res. Lett.*, *24*, 599–602, doi:10.1029/97GL00351.
- Wygant, J. R., et al. (2000), Polar spacecraft based comparisons of intense electric fields and Poynting flux near and within the plasma sheet-tail lobe boundary to UVI images: An energy source for the aurora, *J. Geophys. Res.*, *105*, 18,675–18,692, doi:10.1029/1999JA900500.
- V. Angelopoulos, Institute of Geophysics and Planetary Physics, University of California, 3845 Slichter Hall, Los Angeles, CA 90095, USA.
- U. Auster, Institut für Geophysik und Extraterrestrische Physik, Technischen Universität Braunschweig, D-38106 Braunschweig, Germany.
- J. Bonnell and S. Mende, Space Sciences Laboratory, University of California, 7 Gauss Way, Berkeley, CA 94720, USA.
- J. Bortnik, W. Li, L. R. Lyons, Y. Nishimura, and R. M. Thorne, Department of Atmospheric and Oceanic Sciences, University of California, 405 Hilgard Ave., Los Angeles, CA 90095-1565, USA. (toshi@atmos.ucla.edu)
- C. Cully, Swedish Institute of Space Physics, Box 537, SE-981 28 Uppsala, Sweden.
- R. Ergun, Laboratory for Atmospheric and Space Physics, University of Colorado at Boulder, 1234 Innovation Dr., Boulder, CO 80303-7814, USA.
- O. Le Contel, Laboratoire de Physique des Plasmas, CNRS/Ecole Polytechnique/UPMC/Paris-Sud 11, F-94107 Saint-Maur-des-Fossés CEDEX, France.